

A family of binary magnetic icosahedral quasicrystals based on rare earths and cadmium

Alan I. Goldman^{1,2*}, Tai Kong^{1,2}, Andreas Kreyssig^{1,2}, Anton Jesche^{1,2}, Mehmet Ramazanoglu^{1,2}, Kevin W. Dennis¹, Sergey L. Bud'ko^{1,2} and Paul C. Canfield^{1,2*}

Examples of stable binary icosahedral quasicrystals are relatively rare, and at present there are no known examples featuring localized magnetic moments. These would represent an ideal model system for attaining a deeper understanding of the nature of magnetic interactions in aperiodic lattices. Here we report the discovery of a family of at least seven rare earth icosahedral binary quasicrystals, i-R-Cd (R = Gd to Tm, Y), six of which bear localized magnetic moments. Our work highlights the importance of carefully motivated searches through phase space¹ and supports the proposal that, like icosahedral $\text{Sc}_{12}\text{Zn}_{88}$ (ref. 2), binary quasicrystalline phases may well exist nearby known crystalline approximants, perhaps as peritectically forming compounds with very limited liquidus surfaces, offering very limited ranges of composition/temperature for primary solidification.

Quasicrystals are metallic alloys that manifest aperiodic, rather than periodic, long-range positional order and rotational symmetries (for example, five-fold, ten-fold) that are forbidden for conventional crystals. The formation and stability of quasicrystalline phases, as well as the ways in which aperiodicity modifies electronic, vibrational and magnetic properties, have been intense topics of research over the past 30 years. Stable binary quasicrystalline phases are valuable for studying stabilization mechanisms and the thermodynamics in binary phase diagrams³. Moreover, the discovery of a family of local-moment-bearing binary quasicrystals provides the compositionally simplest system for the study of magnetic interactions in aperiodic compounds.

In support of our discovery of i-R-Cd we have experimentally re-evaluated the Cd-rich regions of the binary R-Cd phase diagrams and have determined the compositions of the deeply peritectic i-R-Cd phases. We further show that these magnetic quasicrystals contain the same basic structural elements, namely Tsai-type rhombic triacontahedral clusters of atoms, as found in the non-moment-bearing i-YbCd_{5,7} icosahedral phase^{3,4} and RCd₆ periodic approximants despite differences in composition. Finally, we present data that strongly suggest that the new quasicrystal phases enter into a low-temperature spin-glass state rather than manifest antiferromagnetic (AFM) order as found for the RCd₆ approximants⁵⁻⁷. The new i-R-Cd system will play a key role as the simplest magnetic quasicrystal system, offering non-magnetic, Y, Heisenberg-like, Gd, and non-Heisenberg (that is, crystal-electric field (CEF) split) Tb to Tm members, as well as the structural and compositional simplicity of a binary phase.

So far, all of the known quasicrystals with moment-bearing elements exhibit frustration and spin-glass-like behaviour at low temperatures^{8,9}. In the ternary i-R-Mg-Zn and i-R-Mg-Cd icosahedral quasicrystals, for example, d.c.- and a.c.-susceptibility

measurements demonstrate spin-glass behaviour¹⁰⁻¹², and neutron diffraction measurements on both i-R-Mg-Zn and i-R-Mg-Cd clearly show the presence of only short-range magnetic correlations at low temperature¹³. Interestingly, the absence of long-range magnetic order also extended to the known crystalline approximant phases as well¹⁴⁻¹⁶. Crystalline approximants are periodic crystals with compositions and unit-cell atomic decorations (for example, atomic clusters) that are closely related to their respective quasicrystalline phases¹⁷. The RCd₆ crystalline phases, which are isostructural to the approximant (YbCd₆) of the non-moment-bearing binary i-YbCd_{5,7} icosahedral phase, provide an exception to this trend because both thermodynamic and scattering measurements have demonstrated the onset of long-range AFM order at low temperatures⁵⁻⁷. The observation of AFM order in the RCd₆ approximants provided a strong impetus to search for and study a related moment-bearing binary icosahedral phase to better understand, or place constraints on, possibilities for the existence of AFM order on an aperiodic lattice¹⁸.

The new i-R-Cd icosahedral family (R = Gd-Tm, Y) was discovered by using solution growth of single crystals^{19,20} as an exploratory synthetic tool. In this case, on the basis of our suspicion that there may be a Cd-rich, quasicrystal phase related to the RCd₆ approximants, we slowly cooled melts of R_{0,07}Cd_{0,93} from 700 °C down to 340 °C and decanted off the remaining (over 99% Cd rich) solution. These first growths revealed large, well-developed crystals of RCd₆ with clear, second-phase, pentagonal dodecahedra, characteristic of solution-grown quasicrystals²⁰, appearing both on the RCd₆ phase as well as on the crucible walls (Fig. 1, inset). Given that the existing R-Cd binary phase diagrams were clearly incomplete on the Cd-rich side of RCd₆ we determined the liquidus line for RCd₆, the peritectic temperature for the quasicrystalline phase, and set limits on the eutectic composition (Fig. 1). With these data we have been able to grow single-phase i-R-Cd by, for example, slowly cooling melts of Gd_{0,008}Cd_{0,992} from 455 °C to 335 °C over 50 h and then decanting off the excess Cd. Even though the exposed liquidus line for i-Gd-Cd formation is small, it shrinks further as we progress from R = Gd to R = Tm; for i-Tm-Cd we could only grow single-phase samples from an initial melt of Tm_{0,006}Cd_{0,994}.

The composition of the icosahedral phase was inferred from two independent methods: wavelength-dispersive X-ray spectroscopy (WDS) and temperature-dependent magnetization (shown in the inset of Fig. 2). Values from each measurement are presented with other magnetic and structural data in Table 1. From the WDS measurements we find an average composition of i-RCd_{7,55±0.3} across the series whereas, from our fits to the high-temperature $H/M(T)$ data for the moment-bearing samples, we find that the composition is slightly more Cd rich: i-RCd_{7,75±0.25}. Both

¹Ames Laboratory, US DOE, Iowa State University, Ames, Iowa 50011, USA, ²Department of Physics and Astronomy, Iowa State University, Ames, Iowa 50011, USA. *e-mail: goldman@ameslab.gov; canfield@ameslab.gov

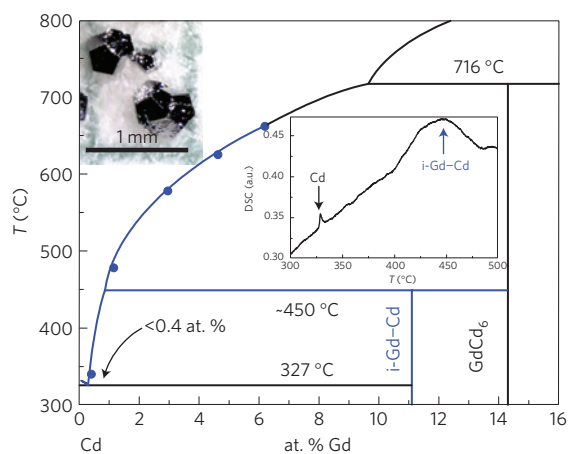


Figure 1 | Revised cadmium-gadolinium binary phase diagram. The Cd-Gd binary phase diagram from ref. 21 is revised (shown in blue) to update the liquidus curve for low Gd concentrations and to include the quasicrystalline phase (labelled i-Gd-Cd). The liquidus curve was re-determined (filled circles) by decanting growths at different temperatures and weighing the crystalline (GdCd₆) or i-Gd-Cd products. Given the mass of starting material, mass of the yield and composition of the crystal, the molar percentage of Gd remaining in the liquid on decant can be calculated. The new eutectic point is inferred to be <math><0.4\%</math> of Gd. The central inset presents the differential scanning calorimetry data from single grains of the quasicrystalline phase taken on warming through their thermal decomposition at roughly 450 °C. The small feature near 320 °C is the melting of the small amount of residual Cd flux on the surfaces of the quasicrystal grains. The pentagonal dodecahedral morphology of the icosahedral phase is shown in the upper-left inset with a millimetre scale; grains as large as ~1.0 mm have been grown.

measurements, however, set compositions for i-R-Cd that: differ significantly from the prototypical YbCd_{5,7} icosahedral quasicrystal and RCd₆ cubic approximants; and are close to the stoichiometry of the recently discovered Sc₁₂Zn₈₈ (ScZn_{7.33} in the present notation) icosahedral phase² as discussed in detail below. We further note that both measurements suggest the possibility of a slight increase in R content for the heavier rare earths relative to R = Gd, which could be driven by steric (ionic size) constraints.

X-ray powder diffraction, using a conventional laboratory source, and high-energy X-ray single-grain diffraction²², using station 6-ID-D at the Advanced Photon Source, were employed to characterize and index the diffraction patterns from several i-R-Cd samples. The single-grain precession images of i-Gd-Cd, shown in Fig. 3a,b, were taken with the beam along a five-fold and two-fold axis of the pentagonal faceted grain and show the pattern of diffraction spots characteristic of a primitive (P-type) quasilattice. This was also confirmed for R = Tb and Tm. Likewise, the diffraction pattern from powdered single grains of i-Gd-Cd, shown in Fig. 3c, is well indexed by a primitive icosahedral quasilattice with a six-dimensional (6D) lattice constant, $a_{6D} = 7.972(4)$ Å. No impurity phases, beyond some residual Cd flux at the <math><5\%</math> level, were found. As the inset of Fig. 3c shows, our powder diffraction measurements for R = Gd, Tb, Dy, Ho, Er and Tm show that a_{6D} decreases smoothly, consistent with the well-known lanthanide contraction.

The difference in composition between the new i-R-Cd phase and the i-YbCd_{5,7} quasicrystal, as well as the RCd₆ quasicrystal approximants, raises the question of whether there are fundamental differences between the structures of these systems. Our analysis of the structure of i-R-Cd relative to the i-YbCd_{5,7} quasicrystal and RCd₆ approximants is based on the close association between the atomic motifs in quasicrystals and their associated approximants¹⁷. The RCd₆ cubic approximants may be described as a body-centred

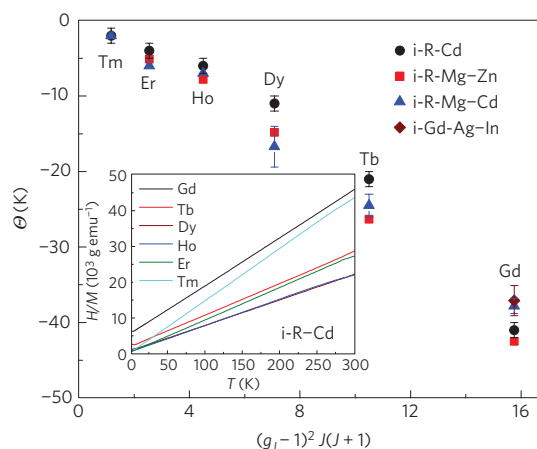


Figure 2 | Weiss temperature, Θ , values versus de Gennes factor. Solid points present the Weiss temperature, Θ , values of i-R-Cd quasicrystals (black circles) obtained from a linear fit of the high-temperature inverse magnetic susceptibility, $\chi^{-1}(T) = H/M(T)$, measured at either $H = 0.5$ or 1 T (shown in the inset). Error bars are inferred from measurements on multiple samples and different fitting ranges. The red, blue and brown symbols represent the Weiss temperature, Θ , values for other icosahedral quasicrystals: i-R₉Mg₃₄Zn₅₇ (ref. 10), i-R₁₀Mg₄₀Cd₅₀ (ref. 11) and i-Gd₁₄Ag₅₀In₃₆ (ref. 15).

Table 1 | Composition, magnetic and structural parameters of the i-R-Cd icosahedral quasicrystals.

RCd _x	x (WDS)	x (Magnetization)	Θ (K)	a_{6D} (Å)
Gd	7.88(18)	7.98(7)	-41(1)	7.972(4)
Tb	7.69(17)	7.89(7)	-21(1)	7.958(4)
Dy	7.50(9)	7.51(6)	-11(1)	7.949(5)
Ho	7.60(13)	7.80(9)	-6(1)	7.935(5)
Er	7.34(13)	7.78(5)	-4(1)	7.935(6)
Tm	7.28(6)	7.76(8)	-2(1)	7.914(5)
Y	7.48(16)	-	-	7.955(5)

The composition of the icosahedral phase as inferred from WDS and temperature-dependent magnetization (Fig. 2, inset), the value of the Weiss temperature, Θ , and the 6D quasilattice constant, a_{6D} , determined by indexing the powder diffraction patterns from each sample (Fig. 3c, inset). The WDS data were calibrated to the values measured for the respective RCd₆ samples we had grown. The R/Cd ratio was also extracted from the temperature-dependent susceptibility by assuming that R = Gd to Tm manifest full, trivalent, local moments and that the temperature-dependent magnetic susceptibility, $\chi(T) = M(T)/H$, could be fitted to a Curie-Weiss law, $\chi(T) = C/(T - \Theta)$. For the heaviest rare earth members of the i-R-Cd series, given the shrinking grain size, the x value inferred from the magnetization data may become less reliable than the WDS value owing to the increasing significance of the small amount of residual Cd flux on the surfaces of the grains. For example, approximately 5% Cd (by mass) second phase on the i-Tm-Cd quasicrystal can shift the inferred value for x from the WDS value of 7.28 to the magnetization-derived value of 7.76. Errors in parenthesis for x from the WDS measurements and a_{6D} represent one standard deviation in the values. The error in x from the magnetization measurements was estimated from fitting over different temperature ranges and weighing errors.

cubic packing of interpenetrating rhombic triacontahedral, or Tsai-type clusters³, which features an icosahedron of 12 R atoms comprising the third shell of the cluster. These clusters, situated at the body-centred cubic lattice points are linked along the cubic axes by sharing a face, and interpenetrate neighbouring clusters along the body diagonal²⁵.

These same clusters have been shown to comprise the backbone of the structure of the icosahedral phase of i-YbCd_{5,7}, with the same type of linkages⁴. Indeed, in terms of the higher dimensional description of aperiodic crystals, the atomic structure of the RCd₆ approximant can be generated by a rational projection of the 6D representation of the icosahedral phase⁴. However, there is only one crystallographic site for the R ion in the approximant structure corresponding to their placement at the vertices of an icosahedron

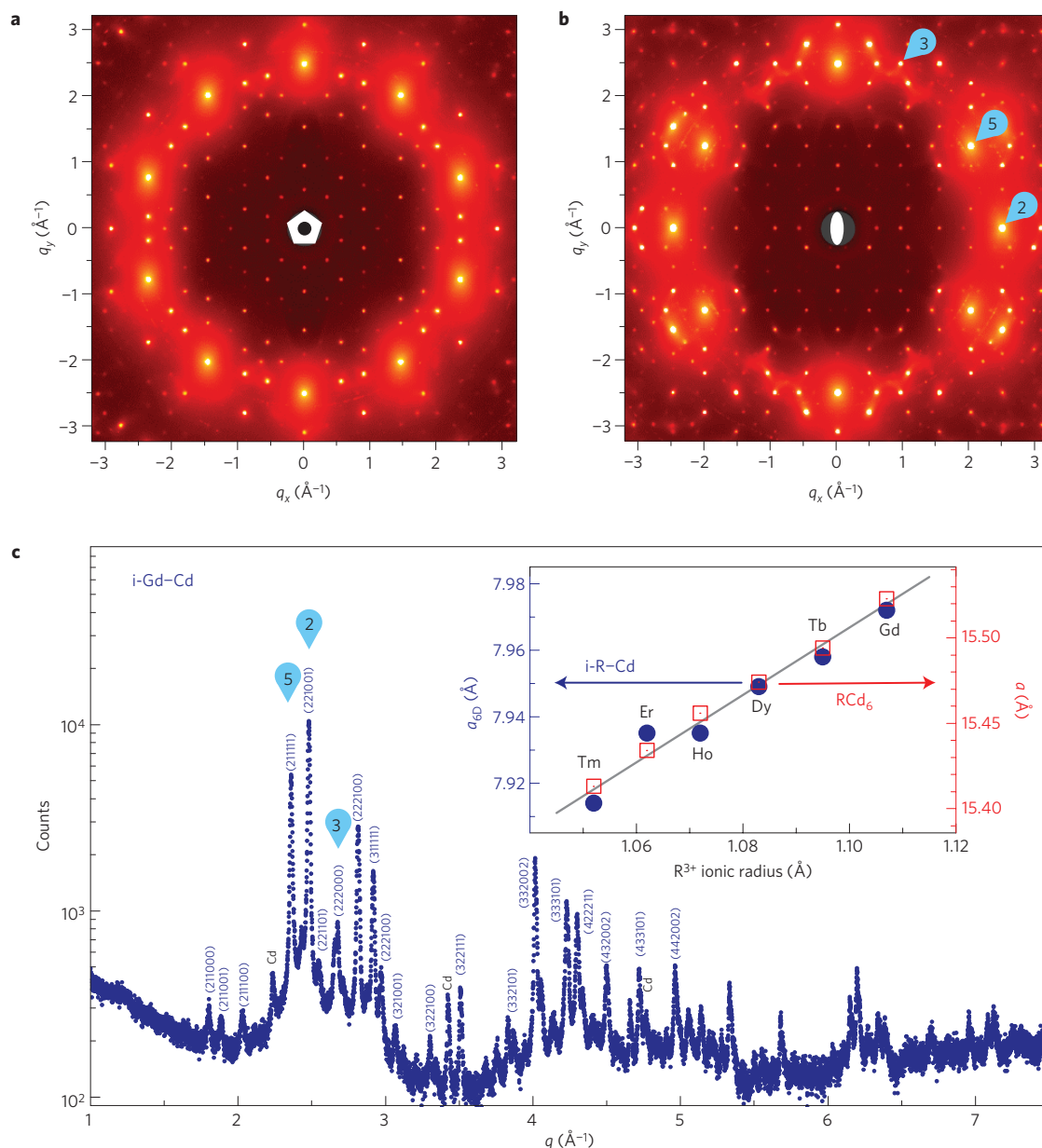


Figure 3 | Single-grain and powder X-ray diffraction from i-Gd-Cd. **a, b**, High-energy X-ray diffraction patterns from a single grain of i-Gd-Cd were taken with the beam parallel to the five-fold (**a**) and two-fold (**b**) axes. The scaling of peak positions along the five-fold axis confirms that the i-Gd-Cd quasicrystals fall within the simple-icosahedral (P-type) structural family. **c**, The powder diffraction pattern from i-Gd-Cd along with the indexing of all peaks for $q < 3 \text{ \AA}^{-1}$, and the prominent peaks for $3 \text{ \AA}^{-1} < q < 5 \text{ \AA}^{-1}$. All peaks in the pattern belong either to the icosahedral phase or the residual Cd flux. The labels 2, 3 and 5 denote prominent peaks along the two-fold, three-fold and five-fold directions, respectively, shown in **b**. The inset shows the scaling of the 6D quasilattice constants (determined from indexing the patterns) for $R = \text{Gd}$ to Tm as a function of ionic radius and compares the lattice constant determined from powder measurements of our RCd_6 samples with the values calculated from a_{6D} as described in the text. Values for the ionic radii were taken from ref. 23 for nine-fold coordination. For i-Y-Cd, the lattice constant for the approximant, derived from $a_{6D} = 7.955 \text{ \AA}$ (15.483 \AA), and the measured value of $a = 15.482 \text{ \AA}$ are also in excellent agreement and lie between those values determined for $R = \text{Dy}$ and Tb . The powder diffraction patterns from the RCd_6 approximants were refined using the Rietveld package GSAS (ref. 24) and the results are in good agreement with the published crystallographic data²⁵.

embedded in the rhombic triacontahedral cluster. For i-YbCd_{5.7}, on the other hand, approximately 70% of the R ions are associated with the embedded icosahedral cluster, whereas 30% are found in the glue that fills the gaps between the rhombic triacontahedral clusters^{4,26}. We propose, as previously suggested²⁷ to explain the low concentration of Sc in i-Sc₁₂Zn₈₈ (ref. 2) and rare earth ions in R-Mg-Cd icosahedral alloys, that the rhombic triacontahedral clusters in i-R-Cd remain intact but the glue filling the gaps between the rhombic triacontahedral clusters is deficient in R ions.

In support of this proposal, we compare our measured value for a_{6D} to the lattice constant, a , expected for the RCd_6 approximant phase through the well-established relation¹⁵: $a = \sqrt{2}a_{6D}(p+q\tau)/\sqrt{(2+\tau)}$, where τ is the golden mean, $((\sqrt{5}+1)/2)$, and p and q are indices that label the approximant. For the case at hand, $p = q = 1$. For i-Gd-Cd, we find a calculated value of $a = 15.519(6) \text{ \AA}$, in excellent agreement with our measured lattice parameter for GdCd_6 of $15.523(5) \text{ \AA}$. As the inset of Fig. 3c shows, excellent agreement between the derived and measured

cubic approximant lattice constants is found for all R ions in the i-R–Cd family. This provides compelling evidence that, despite rather significant differences in composition, the cluster-based backbone of the icosahedral structure of the i-R–Cd quasicrystal is quite similar, if not identical, to that found for i-YbCd_{5.7} and the RCd₆ cubic approximants. Full confirmation of this proposal, however, will require a full 6D structural refinement of the i-R–Cd quasicrystal as was done for i-YbCd_{5.7} (ref. 4).

We now turn to the detailed magnetic properties of the i-R–Cd quasicrystals, particularly in comparison with their AFM-ordered RCd₆ cubic approximants. We begin by returning to the high-temperature $H/M(T)$ measurements shown in Fig. 2. From these data, the Weiss temperature, θ , is shown together with values previously measured for other ternary rare-earth-containing quasicrystalline compounds including i-R₉Mg₃₄Zn₅₇ (ref. 10), i-R₁₀Mg₄₀Cd₅₀ (ref. 11) and i-Gd₁₄Ag₅₀In₃₆ (ref. 15). For all of these compounds, θ is negative, denoting predominantly AFM exchange interactions, and roughly scales with the de Gennes factor, as expected. What is most striking, however, is that the values for θ are very consistent from system to system even though these compounds manifest different compositions and structural classes. i-R₉Mg₃₄Zn₅₇, for example, is a ternary face-centred (F-type) icosahedral quasicrystal characterized by Bergman-type clusters, whereas we have now shown that i-R–Cd is a binary P-type icosahedral quasicrystal characterized by rhombic triacontahedral clusters. Nevertheless, the strength of the AFM exchange, characterized by θ , and its monotonic dependence on the de Gennes factor, remains remarkably similar across the spectrum of structures. This may simply be a consequence of the presence, in all cases, of a similar electronic environment associated with the Hume–Rothery mechanism for the stabilization of quasicrystals²⁸ or from close similarities in the local environments of the R ions for all of these structures. Clearly, this point deserves further experimental and theoretical study.

To further explore the low-temperature magnetic state of i-R–Cd we show the field-cooled (FC) and zero-field-cooled (ZFC) $M(T)/H$ data for i-Gd–Cd, i-Tb–Cd and i-Dy–Cd in Fig. 4. These data suggest that the quasicrystalline phase, for R = Gd, Tb and Dy, enters into a low-temperature spin-glass state. i-Gd–Cd exhibits canonical spin-glass behaviour where there is a pronounced difference between the FC and ZFC data below a peak that can be clearly identified with a spin-freezing temperature²⁹, $T_f = 4.6$ K. For R = Gd, T_f is almost a factor of ten smaller than θ , consistent with values typical for strongly frustrated systems. The data for R = Tb and Dy seem to be more complicated. For both samples, the separation of the FC and ZFC curves occurs at higher temperature than the peak in the ZFC magnetization. This observation is not unique to these binary quasicrystals, as it has also been noted in the Tb–Mg–Cd system^{11,12}, and has been subject to several interpretations including the presence of a distribution of spin-freezing temperatures and/or the onset of short-range magnetic correlations above T_f (ref. 13), and CEF effects. The different behaviour noted for i-Gd–Cd is of particular interest in this context because it is an S-state ion, which does not manifest any CEF anisotropy. Similar magnetization measurements on i-Ho–Cd, i-Er–Cd and i-Tm–Cd do not evidence FC/ZFC differences or signatures of magnetic ordering above $T = 2$ K, the lowest temperature that could be reached in the present measurements. We find the magnetic behaviour of the i-R–Cd phase is in stark contrast to what is observed for the closely related RCd₆ approximants (Fig. 4), where signatures that have been associated with long-range magnetic order are clearly seen^{5–7}.

Given the greater structural and chemical simplicity associated with a binary compound, the matched sets of i-R–Cd and RCd₆ for R = Gd–Tm form model systems that will allow us to determine, refine and test our understanding of the key

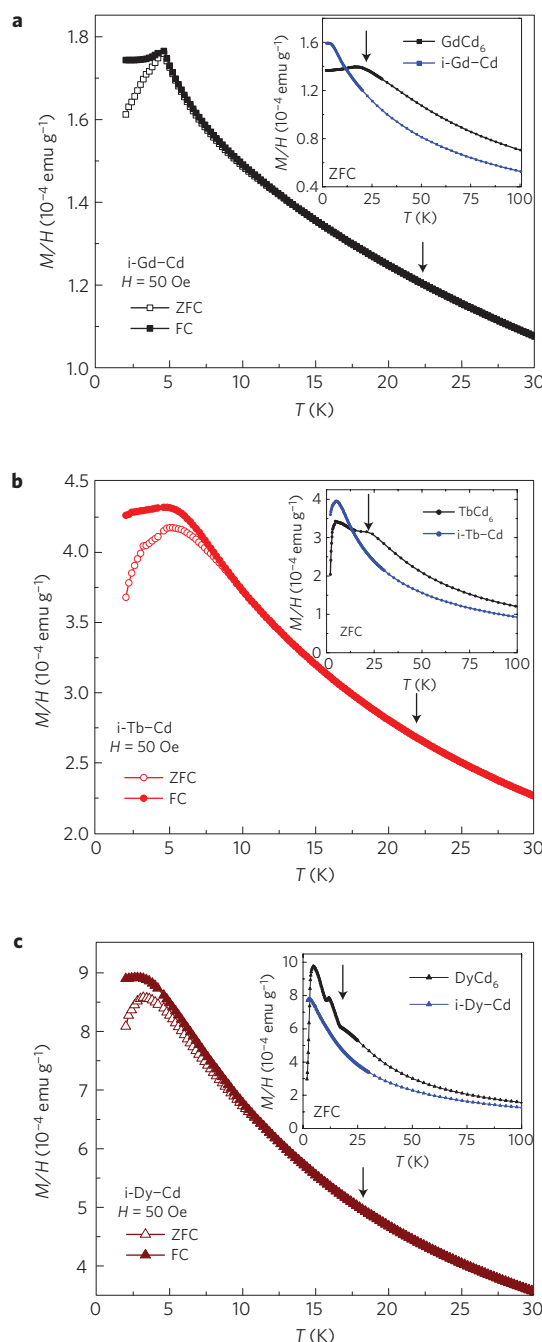


Figure 4 | Low-temperature FC and ZFC magnetic susceptibility, $M(T)/H$, data. **a–c**, Temperature-dependent FC and ZFC magnetization data measured at 50 Oe from i-Gd–Cd (**a**), i-Tb–Cd (**b**) and i-Dy–Cd (**c**). The insets compare the higher-field $M(T)/H$ data (ZFC) for icosahedral phase samples with their respective RCd₆ approximants. The arrows in the insets indicate the location of clear magnetic ordering features for the RCd₆ approximants^{5–7}, which are absent for the related i-R–Cd compounds (main figure).

features and properties associated with quasicrystalline structure and magnetism. Structurally, the i-R–Cd series presents the intriguing prospect of two very different quasicrystal compositions associated with the same approximant, possibly with very different R content in the glue. Magnetically, the i-R–Cd series, coupled with its AFM-ordering RCd₆ approximants, allows for direct comparisons between the low-temperature magnetic states of crystalline and quasicrystalline phases with fundamentally similar

R-based clusters. Our results, so far, support the idea that the presence of aperiodic, rather than periodic, order disrupts or frustrates long-range magnetic order.

Methods

Single-grain quasicrystals were grown out of Cd-rich binary solutions. A typical procedure involved adding approximately 5 g of Cd (Alfa Aesar, 99.9999% purity) and 0.06 g of rare earth elements (Ames Lab) into a 2 ml alumina crucible with a molar ratio of Cd/R = 99.2:0.8 (R = Y, Gd–Dy) or 99.4:0.6 (R = Ho–Tm). The crucible with the starting elements was sealed in a fused-silica ampoule under a partial argon atmosphere, which was then heated up to 700 °C, held at 700 °C for 10 h, cooled to 455 °C in 3 h and then slowly (roughly 2 °C h⁻¹) cooled to 335 °C, at which temperature the R-depleted, remaining Cd-rich solution was decanted with the assistance of a centrifuge. Clusters of single grains with a mass of about 0.2 g were obtained from each growth.

Elemental analysis was performed using WDS in the electron probe microanalyser of a JEOL JXA-8200 electron microprobe with a 20 kV beam voltage and a 5- μ m spot size. For each sample, the measurement was done at 12 different locations on a polished surface. Differential thermal analysis was performed on samples sealed in tantalum capsules under high-purity argon using a Miyachi/Unitek pulsed laser system allowing welding of the capsule with little or no sample heating. Calorimetry was performed on a Netzsch 404C using baseline background subtraction and a heating rate of 10 K min⁻¹.

Powder X-ray diffraction patterns were measured on a Rigaku Miniflex II desktop X-ray diffractometer (Cu K α radiation). Samples were prepared by grinding single grains into powder, which were then mounted and measured on a Si single-crystal zero-background sample holder. High-energy X-ray diffraction measurements were performed on station 6-ID-D at the Advanced Photon Source using 100 keV X-rays and an area detector (MAR 345) positioned 98 cm from the sample position. Data were taken in precession mode where the axis normal to the reciprocal lattice planes of interest is set at a small, but finite, half-cone angle with respect to the incident beam direction and rotated about it.

The d.c. magnetization measurements were performed in a Quantum Design Magnetic Property Measurement System (MPMS-5), superconducting quantum interference device magnetometer ($T = 1.8$ –350 K, $H_{\text{max}} = 5.5$ T). Low-field (50 Oe) magnetization was measured on warming for ZFC, and on cooling for FC data.

Received 27 February 2013; accepted 26 April 2013;
published online 9 June 2013

References

- Canfield, P. C. Fishing the Fermi sea. *Nature Phys.* **4**, 167–169 (2008).
- Canfield, P. C. *et al.* Solution growth of a binary icosahedral quasicrystal of Sc₁₂Zn₈₈. *Phys. Rev. B* **81**, 020201(R) (2010).
- Tsai, A. P., Guo, J. Q., Abe, E., Takakura, H. & Sato, T. J. A stable binary quasicrystal. *Nature* **408**, 537–538 (2000).
- Takakura, H., Pay Gómez, C., Yamamoto, A., De Boissieu, M. & Tsai, A. P. Atomic structure of the binary icosahedral Yb–Cd quasicrystal. *Nature Mater.* **6**, 58–63 (2007).
- Tamura, R., Muro, Y., Hiroto, T., Nishimoto, K. & Takabatake, T. Long-range magnetic order in the quasicrystalline approximant Cd₆Tb. *Phys. Rev. B* **82**, 220201(R) (2010).
- Kim, M. G. *et al.* Antiferromagnetic order in the quasicrystal approximant Cd₆Tb studied by X-ray resonant magnetic scattering. *Phys. Rev. B* **85**, 134442 (2012).
- Mori, A. *et al.* Electrical and magnetic properties of quasicrystal approximants RCd₆ (R: rare earth). *J. Phys. Soc. Jpn* **81**, 024720 (2012).
- Fukamichi, K. *Physical Properties of Quasicrystals* 295–326 (Springer, 1999).
- Hippert, F. & Prejean, J. J. Magnetism in quasicrystals. *Phil. Mag.* **88**, 2175–2190 (2008).
- Fisher, I. R. *et al.* Magnetic and transport properties of single-grain R–Mg–Zn icosahedral quasicrystals (R = Y, Y_{1-x}Gd_x, Y_{1-x}Tb_x, Tb, Dy, Ho, and Er). *Phys. Rev. B* **59**, 308–321 (1999).
- Sato, T. J., Guo, J. Q. & Tsai, A.-P. Magnetic properties of the icosahedral Cd–Mg–rare-earth quasicrystals. *J. Phys. Condens. Matter* **13**, L105 (2001).

- Sebastian, S. E., Huie, T., Fisher, I. R., Dennis, K. W. & Kramer, M. J. Magnetic properties of single grain R–Mg–Cd primitive icosahedral quasicrystals (R = Y, Gd, Tb or Dy). *Phil. Mag.* **84**, 1029–1037 (2004).
- Sato, T. J. Short-range order and spin-glass-like freezing in A–Mg–R (A = Zn or Cd; R = rare-earth elements) magnetic quasicrystals. *Acta Crystallogr. A* **61**, 39 (2005).
- Jazbec, S. *et al.* Geometric origin of magnetic frustration in the μ -Al₁₃Mn giant-unit-cell complex intermetallic. *J. Phys. Condens. Matter* **23**, 045702 (2011).
- Wang, P., Stadnik, Z. M., Al-Qadi, K. & Przewoźnik, J. A comparative study of the magnetic properties of the 1/1 approximant Ag₅₀In₃₆Gd₁₄ and the icosahedral quasicrystal Ag₅₀In₃₆Gd₁₄. *J. Phys. Condens. Matter* **21**, 436007 (2009).
- Ibuka, S., Iida, K. & Sato, T. J. Magnetic properties of the Ag–In–rare-earth 1/1 approximants. *J. Phys. Condens. Matter* **23**, 056001 (2011).
- Goldman, A. I. & Kelton, K. F. Quasicrystals and crystalline approximants. *Rev. Mod. Phys.* **65**, 213–230 (1993).
- Lifshitz, R. Symmetry of magnetically ordered quasicrystals. *Phys. Rev. Lett.* **80**, 2717–2720 (1998).
- Canfield, P. C. *Properties and Applications of Complex Intermetallics* 93–111 (World Scientific, 2010).
- Canfield, P. C. & Fisher, I. R. High-temperature solution growth of intermetallic single crystals and quasicrystals. *J. Cryst. Growth* **225**, 155–161 (2001).
- Gschneidner, K. A. Jr & Calderwood, F. W. in *Binary Alloy Phase Diagrams* 2nd edn Vol. 2 (ed. Massalski, T. B.) 980–983 (1990).
- Kreyssig, A. *et al.* Crystallographic phase transition within the magnetically ordered state of Ce₂Fe₁₇. *Phys. Rev. B* **76**, 054421 (2007).
- Shannon, R. D. Revised effective ionic radii and systematic study of interatomic distances in halides and chalcogenides. *Acta Crystallogr. A* **32**, 751–767 (1976).
- Larson, A. C. & Von Dreele, R. B. General Structure Analysis System (GSAS), *Los Alamos National Laboratory Report LAUR 86-748*, (2004).
- Pay Gómez, C. & Lidin, S. Comparative structural study of the disordered MCd₆ quasicrystal approximants. *Phys. Rev. B* **68**, 024203 (2003).
- Kawana, D., Watanuki, T., Machida, A., Shobu, T. & Aoki, K. Intermediate-valence quasicrystal of a Cd–Yb alloy under pressure. *Phys. Rev. B* **81**, 220202(R) (2010).
- Tsai, A.-P. Discovery of stable icosahedral quasicrystals: Progress in understanding structure and properties. *Chem. Soc. Rev.* <http://dx.doi.org/10.1039/C3CS35388E> (2013).
- Janot, C. *Quasicrystals: A Primer* (Oxford Univ. Press, 1992).
- Mydosh, J. A. *Spin Glasses: An Experimental Introduction* (Taylor and Francis, 1993).

Acknowledgements

We acknowledge and thank W. Straszheim for the WDS measurements, D. S. Robinson and A. Sapkota for assistance with the high-energy X-ray diffraction measurements and R. J. McQueeney for useful discussions. The research was supported by the Office of the Basic Energy Sciences, Materials Sciences Division, US Department of Energy (DOE). Ames Laboratory is operated for DOE by Iowa State University under contract No. DE-AC02-07CH11358. Use of the Advanced Photon Source was supported by the US DOE under Contract No. DE-AC02-06CH11357.

Author contributions

A.I.G., P.C.C., S.L.B. and A.K. designed the measurements; T.K., S.L.B. and P.C.C. grew the samples, and performed and analysed the magnetization measurements; K.W.D. performed the differential thermal analysis measurements and analysis; T.K., A.J., M.R., A.K. and A.I.G. performed the X-ray diffraction measurements and data analysis. A.I.G. and P.C.C. drafted the manuscript and all authors participated in the writing and review of the final draft.

Additional information

Reprints and permissions information is available online at www.nature.com/reprints. Correspondence and requests for materials should be addressed to A.I.G. or P.C.C.

Competing financial interests

The authors declare no competing financial interests.